Title: Biomass-based composite catalysts for catalytic wet peroxide oxidation of bisphenol A: preparation and characterization studies

Authors: Riikka Juhola, Anne Heponiemi, Sari Tuomikoski, Tao Hu, Hanna Prokkola, Henrik Romar, Ulla Lassi

PII: S2213-3437(19)30250-7
DOI: https://doi.org/10.1016/j.jece.2019.103127
Article Number: 103127

Reference: JECE 103127

To appear in:

Received date: 18 January 2019
Revised date: 23 April 2019
Accepted date: 28 April 2019

Please cite this article as: Juhola R, Heponiemi A, Tuomikoski S, Hu T, Prokkola H, Romar H, Lassi U, Biomass-based composite catalysts for catalytic wet peroxide oxidation of bisphenol A: preparation and characterization studies, *Journal of Environmental Chemical Engineering* (2019), https://doi.org/10.1016/j.jece.2019.103127

Biomass-based composite catalysts for catalytic wet peroxide oxidation of bisphenol A: preparation and characterization studies

Riikka Juhola[1], Anne Heponiemi[1], Sari Tuomikoski[1], Tao Hu[1], Hanna Prokkola[1], Henrik Romar[1,2], Ulla Lassi[1,2]

[1] – University of Oulu, Research Unit of Sustainable Chemistry, P.O. Box 4300, FI-90014 University of Oulu, Finland

[2] – University of Jyväskylä, Kokkola University Consortium Chydenius, P.O. Box 567, FI-67701 Kokkola, Finland

*Corresponding author: ulla.lassi@oulu.fi, +358 400 294 090

Graphical Abstract

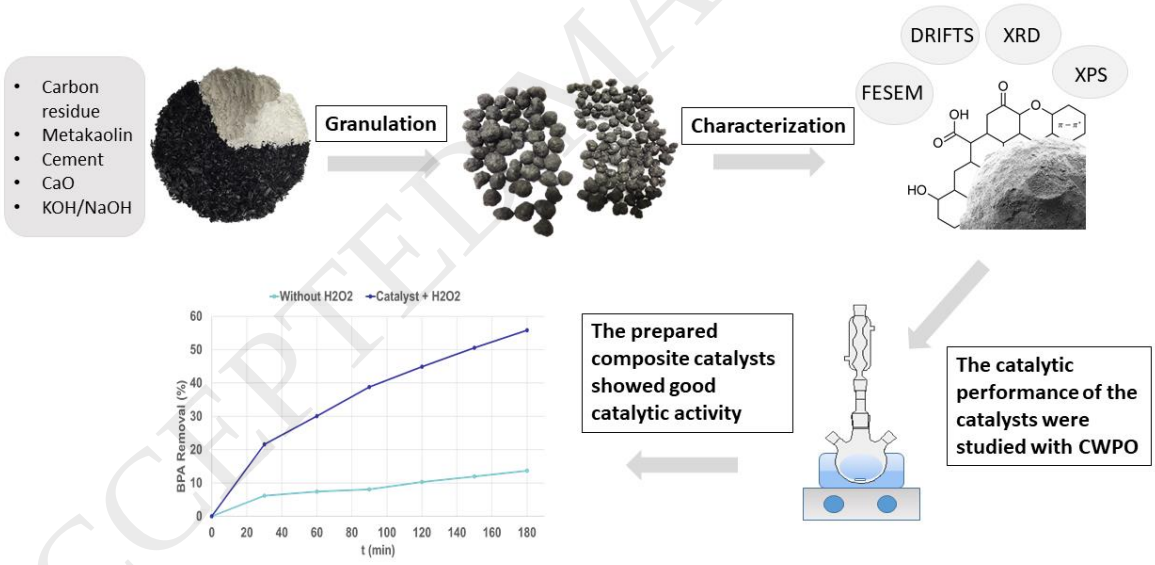

Highlights

- The optimized conditions for the granulation of biomass-based carbon were studied
- Carbon combined with metakaolin, CaO and NaOH produced stable composite granules

- The most stable composites were tested in catalytic wet peroxide oxidation of BPA
- The catalytic activity of composites was higher than powdered carbon raw material
- Catalytic activity is based on surface functionality and basicity of composites

Abstract

The wet granulation process was used to prepare new, efficient, and cost-effective granular biomass-based composite catalysts for catalytic wet peroxide oxidation (CWPO) of bisphenol A (BPA). The most stable composite granules was prepared by mixing biomass-based carbon residue (CR) with metakaolin (MK) combined with calcium oxide (CaO) or cement and a solvent (NaOH or KOH). For all the prepared composite granules, the optimized binding agents to carbon ratio was 0.3, the solvent to carbon ratio 1.2, and the agitation rate 1200 rpm. The specific surface area of the prepared catalysts was 152–205 m^2/g. The composite granular catalyst (CR+MK+CaO+NaOH) had the most durable and stable structure (compressive strength of 27 N) and the most basic surface (15 mmol/g) measured with temperature programmed desorption. This catalyst was the most active in CWPO of BPA and total organic carbon removal of 50% and 48%, respectively.

Keywords

Biomass, Granular activated carbon, wastewater purification, Composite catalyst, Oxidation of bisphenol A

1 Introduction

Carbon materials, such as granular activated carbon (GAC), have been used in heterogeneous catalysis as a support material and as a catalyst material on their own [1-6]. Commercial GAC has been acknowledged as an excellent material for removing low-solubility contaminants (such as phenolic compounds from wastewater) [4, 5, 7], but a major disadvantage is the high price. In contrast, the utilization of waste biomass residues, such as seeds [8, 9], wood [10, 11], and fruit stones [12, 13], in activated carbon has become very popular for several reasons: the unwanted waste can be used as value-added materials (e.g., catalysts), waste is typically inexpensive and comes from renewable sources. To enhance these materials to have similar or even better characteristics than their commercial counterparts is preferred [14]. Using granules instead of powder has many advantages: The production with an uniform composition, separation from the liquid phase after use, ease of reuse and regeneration, the improved flow properties and lack of dust problems [15-17]. These advantages are the main motivations to develop porous, stable, and eco-friendly biomass-based granular composite catalyst materials for water purification.

Structuring materials in the form of granules is not new, but limited open scientific research has been published. Depending on the characteristics of the raw material, GAC can be produced directly, from hard raw materials (e.g., nutshells and grape seeds) [8, 18, 19], or indirectly, from low-hardness raw materials (e.g. wood) using adequate binders [20-22]. Typically, inorganic binders (e.g. alumina, cement, silica, and clay) or organic binders (e.g. starch and sugar) improve the mechanical strength and the porosity of the material [20-23]. However, the

use of cement is not always desired as its production emits a high amount of CO_2 and consumes a lot of energy whereas organic binders might leach out in use [23]. The so-called pozzolanic binder materials (i.e., siliceous and aluminous materials like metakaolin) are highly reactive materials [24]. Metakaolin has also been used as a heterogeneous catalyst material [25, 26] and as an adsorbent [27]. The versatility of metakaolin arises from its high strength and resistance to high temperatures and chemicals [28], which, in turn, are the result of the material's structure: a three-dimensional network of AlO_4 and SiO_4 tetrahedral units connected by oxygen corners. Therefore, to form stable granular composites with the necessary strength, metakaolin could be combined with biomass-based waste material. To obtain high catalytic activity in a catalytic wet peroxide oxidation (CWPO), it is imperative that the structural and textural properties of GAC are suitable. The heterogeneous surface chemistry of carbon materials has been long acknowledged; the active surface sites are capable of chemisorbing the reactants and forming surface intermediates of adequate strength [29-31]. Furthermore, the surface chemistry can be tailored. The basic surface groups, such as the π-electron system of the basal planes and quinone type structures, and the basicity of the reaction media have shown a positive effect toward the catalytic performances in CWPO, by enhancing the decomposition of H_2O_2 [12, 32]. Use of alkaline earth metal oxides, such as calcium oxide (CaO), could bring basic, highly reactive species (O^{2-}) on the carbon surface [33], which, in turn, readily react with water, for example, to generate hydroxide ions to the reaction media, therefore, providing the basic environment for the CWPO reaction. Moreover, CaO is commonly used in the preparation of cementless materials, as CaO has been shown to greatly enhance the dissolution of aluminosilicates, such as metakaolin, which, in turn, results in higher strength [34].

In this study, new biomass-based granular composite materials were prepared by combining waste biomass residues, metakaolin, and CaO with either NaOH or KOH to obtain mechanically strong and catalytically active materials. For comparison, composite materials with cement were also prepared. The optimal conditions for the wet granulation process of biomass-based carbon were analyzed to identify its possible use as an ecological granular composite catalyst material for CWPO of BPA. The composites were characterized using several techniques, e.g. temperature programmed desorption (TPD), diffuse reflectance infrared radiation Fourier transform spectroscopy (DRIFTS) and X-ray photoelectron spectroscopy (XPS).

2 Experimental

2.1 Materials

The studied biomass-based materials were willow carbon (CW) carbonized at around 400-500 ℃ (material obtained from a Finnish company, pilot-scale willow-carbon production process) and carbon residue (CR, a mixture of pine and birch tree) formed in the biomass gasification process at around 1000 °C. The binders used were commercial cement (Finnsementti, including Portland cement 65–79%, blast furnace slag 0–25%, and limestone 6–15%), CaO (Riedel-de-Haën), and metakaolin (Aquaminerals Finland Ltd., including Al_2O_3 40.3%, SiO_2 53.1%, K_2O 2.72%, and Fe_2O_3 1.89% [35]), and solvents 5 M potassium hydroxide (Merck) or 5 M sodium hydroxide (Merck). The HCl (FF-Chemicals) and NaOH (FF-Chemicals) solutions used for Boehm titrations were standard titration solutions, whereas $NaHCO_3$ (Merck), Na_2CO_3 (100%, VWR Chemicals), bisphenol A (Sigma-Aldrich), H_2O_2 (30% w/w, Merck), H_2SO_4 (J.T. Baker), and NaCl (VWR Chemicals) were reagent grade. The carbon and binder materials were in powder form (particle size < 150 µm).

2.2 Pretreatment of carbon materials

Before the experiments, the willow carbon and carbon residue were washed with a 1 N solution of HCl:H_2SO_4 for 24 h by using a liquid to solid ratio of 10 (W/W). The samples were filtered and washed with distilled water using a liquid to solid ratio of 40 (W/W) for 1 h. Also, materials that were not acid washed, named CW 4 and CR4, were used for the granulation. After washing several times with distilled water until neutral pH. The samples were filtered and dried overnight at 105 °C before granulation.

2.3 Preparation of the carbon composite granules

The wet granulation process was conducted using a rotary drum granulator (Eirich laboratory EL1). The combination of the binding agents mixed with the carbon as well as solvent and the nomenclature are presented in Table 1. The carbon material and binding agents were weighed, mixed, and put in the granulation mixer. The solvent was added gradually to obtain an effective wetting. The agitation rate was 1200 rpm.

2.4 Studying the stability and mechanical strength of the composite granules

The stability of the composite granules was studied at 20 °C in water without mixing and with mixing (300 rpm) overnight. Then the composite granules were put in water and heated until boiling. The most stable composite granules were then studied in water in CWPO reaction conditions, at 50 °C for 3 h (500–700 rpm). Mechanical strength tests were run using the Zwick Z100 Roell testing machine with TestXpert II software on day 1, 7, and 28 after preparation. The composite granules were stored in closed bottles at room temperature. A granule diameter of 3–4 mm (sieved) was used. The composite granule was loaded under a constant deformation rate of 0.01 mm/s. From each batch, 10 granules were studied, and the average compressive strengths were calculated. Before the characterization and oxidation experiments, the stable granules were calcined under nitrogen gas flow (2 L/min) for 5 h at 280 °C.

2.5 Characterization

2.5.1 Ultimate analysis, morphological structure, and N_2 adsorption-desorption

The metal content of the CR and composite granules was measured with inductively coupled plasma optical emission spectroscopy (ICP-OES, Perkin Elmer Optima 5300 DV), and the elemental analysis of the samples was carried out in a Flash 2000 organic elemental analyzer (Thermo Scientific with Eager Xperience software) to determine the C and O content in a stream of pure O_2 and He, respectively. The surface morphology of the samples was investigated using a Zeiss ULTRA plus field emission scanning electron microscopy (FESEM) combined with energy-dispersive X-ray spectroscopy (EDS) for the element analysis. The porosity of the samples was determined from nitrogen adsorption-desorption isotherms at the temperature of liquid nitrogen (–196 °C), using a Micromeritics ASAP 2020 (Norcross). The specific surface areas and the pore volumes were calculated using Brunauer-Emmett-Teller (BET) and Barrett-Joyner-Halenda (BJH) equations [36], and the pore size distribution was calculated using density functional theory (DFT) [37].

2.5.2 Boehm titration

The content of probable acidic surface functional groups of the prepared composite granules was determined with Boehm titration [38]. Base solutions of $NaHCO_3$, Na_2CO_3, and NaOH (0.05 M) were prepared in deionized water. 25 mL of the base solutions were added to 0.15 g of granules in 50 mL polyethylene flasks, placed on a laboratory shaker at room temperature for 48 h. Samples were filtrated and 10 mL aliquots of the filtrate were acidified with the 0.05 M HCl solution. For the neutralization of NaOH and $NaHCO_3$, 20 mL of HCl was used, whereas for Na_2CO_3, 30 mL of HCl was used for the neutralization. All samples were then titrated with the 0.05 M NaOH solution, and the endpoint at pH 7 was determined potentiometrically. Surface functional groups were quantified by assuming that NaOH neutralizes carboxylic, lactonic, and phenolic groups, Na_2CO_3 neutralizes carboxylic and lactonic groups, and $NaHCO_3$ neutralizes only carboxylic groups.

2.5.3 pH and point of zero charge measurement

The pH of the materials (0.15 g) was determined in water suspension (12.5 mL) after heating at 90 °C and then cooling to room temperature. The so-called pH drift method was used to determine the bulk total surface charge (pH_{pzc}) [39]. The 0.001 M NaCl solution was first bubbled with nitrogen, and then the deoxygenized solution (50 mL) was combined with 0.15 g of materials. After that, the pH of the aqueous suspension was adjusted between 2 and 14, and the suspensions were stirred for 48 h. Then the final pH was measured. The pH_{pzc} was determined at the value where pH_{final} intercepted $pH_{initial}$.

2.5.4 Temperature programmed desorption

The basicity of the s materials was measured with TPD of CO_2 with an AutoChem II 2920 device. Before the CO_2 TPD analysis, the sample was flushed with H_2 (30 mL/min) from room temperature to 550 °C at 10 °C/min for 30 min, cooled to 50 °C, and flushed with Ar at 50 mL/min for 5 min. The 5% CO_2/Ar (50 mL/min) was adsorbed at 50 °C for 60 min, and then the physisorbed CO_2 was flushed with Ar (50 mL/min) at 50 °C for 30 min. The thermodesorption of CO_2 was performed with Ar (50 mL/min) from 50 °C to 950 °C and left for 10 min at this temperature. The temperature rate for CO_2 TPD was 10 °C/min.

2.5.5 X-ray diffraction

The crystalline phase identification of the materials was studied using XRD (PANalytical X'Pert Pro) with the monochromatic Cu Kα1 (λ=1.5406 Å) at 45 kV and 40 mA with a scan speed of 0.02 degrees/s and 2θ ranging from 10° to 80°. The diffractograms were compared to the Powder Diffraction File standards from the International Centre for Diffraction DATA (ICDD).

2.5.6 Spectroscopic measurements

The surface functional groups of the samples were studied with DRIFTS (Brüker PMA 50 Vertex 80V) at room temperature in ambient atmosphere. Samples were diluted with KBr (1:100). The sample chamber was purged with nitrogen (100 mL/min). The spectra were recorded in the range of 4000–400 1/cm. XPS was recorded with an ESCALAB 250 Xi XPS System (Thermo Fisher Scientific). The X-ray excitation was provided by a monochromatic Al Kα (1486.6 eV) source. The C, O, Ca, Al, Si, Na, and K contents were measured for all samples. The measurement data was analyzed with the Thermo Avantage program. Charge

compensation of the binding energies (BEs) was performed by applying the C1s line at 284.8 eV as a reference.

2.6 Catalytic studies

The preliminary catalytic wet peroxide oxidation experiments of BPA aqueous solution (60 mg/L) were performed for the most stable composite granules (catalyst diameter < 2 mm). The initial pH of the medium was found between 9 and 11 for the granules and between 5 and 6.5 for CR, and the catalyst loading was kept constant at 1 g/L. The amount of hydrogen peroxide needed for complete mineralization of the organic carbon was estimated to be 5.6 times the mass ratio of H_2O_2/BPA (Eq. 1):

$$C_{15}H_{16}O_2 + 36\ H_2O_2 \rightarrow 15\ CO_2 + 44\ H_2O. \quad (1)$$

The oxidation reaction was carried out in water bath in a three-necked 500 mL round bottom flask, equipped with a magnetic stirrer and a reflux condenser. The powdered carbon residue or granular composite catalyst (1 g/L) was introduced into 160 mL of an aqueous BPA solution (60 mg/L) under continuous stirring. The experiments were run at 50 °C and the initial pH for 3 h. After the temperature was stabilized, a solution of 0.15% H_2O_2 was added to the reactor, which was taken as the starting point of the reaction (t = 0). H_2O_2 was added during the experiment in doses (1.5 g/L) with the stoichiometric amount of the H_2O_2/BPA. Samples were taken periodically and filtered through 0.45 μm filter paper. The dissolved oxygen content and the pH (Hach Lange HQ40d portable meter, LDO and pH probes) were investigated during the experiment. The possible adsorption of BPA on the catalyst surface was studied using the same reaction conditions but without the addition of the oxidizing agent, H_2O_2. The activity was followed by measurement of the total organic carbon (TOC).

2.6.1 Stability tests

The stability of the catalytically most active granular composite catalyst was further studied with CWPO experiments conducted in two consecutive runs. The catalyst was recovered with hot filtration from the solution after the catalytic experiment, washed with distilled water and dried at 105 °C overnight, and then tested again in the same reaction conditions.

2.6.2 Analytical methods

The concentration of BPA was detected with high-pressure liquid chromatography (HPLC) equipped with an ultraviolet-visible (UV-VIS) detector, using a 226 nm wavelength (Shimadzu SPD-10A). A mixture of 0.1% trifluoroacetic acid (TFA) in water and 0.1% TFA in methanol was used as the eluent (flow rate 0.4 mL/min), and the compounds were separated with the SunFire™ C18 5 m 2.1 × 100 mm column, operated at a temperature of 30 °C. Mineralization of the TOC was measured in the BPA samples by using the Skalar Formacs^{HT} Total Organic Carbon/Total Nitrogen analyzer. The amount of possible leached metals (Ca and Al) after the oxidation reactions was detected with ICP-OES (Perkin Elmer Optima 5300 DV).

3 Result and Discussion

The goal of the research was first, to study the preparation of mechanically stable materials, second, to learn in more detail the characteristics of the as-prepared materials, and third, to study the activity of these materials in CWAO of BPA.

3.1 Stability and mechanical strength of the composite granules

The surface porosity and mechanical strength are summarized in Table 2 with comparison of acid washed CR. The specific surface area (SSA) of the composite granules decreased when compared to the powder CR. The SSA was relatively high with no major difference between granules. CR2 and CR4 were found to be mainly micro- and mesoporous whereas CR3 also had some macroporosity, which is probably due to the formation of hydration products. The different porosity profile of CR3 might also be the reason for the lower mechanical strength as the strength of the granules depends not only on the attractive forces between the particles and the porosity but also of the size of the largest pores [23].

Only carbon residue samples were stable due to the structural difference between CR and willow carbon. However, one composite granule prepared from carbon residue, sample CR1, did not pass the stability test. CR1 was prepared by combining acid washed carbon residue, CaO, and metakaolin using KOH as the solvent. Sample CR2, prepared in a similar way except the solvent used was NaOH passed the stability tests. Similar results have been found in other studies [40, 41], that a higher extent of metakaolin affects to the stability and mechanical strength when the NaOH solution is used instead of the KOH solution. The latter is known to increase gel formation by association with aluminosilicate anions whereas sodium cations increase amorphous phase dissolution by association with silicate monomers [42].

The other stable composite granules, CR3 and CR4, were prepared by mixing acid washed carbon residue or carbon residue without acid washing, metakaolin, and cement with KOH or NaOH, respectively. The stability, in this case, is most likely due to the cement that contributes to the strength probably by space-filling as the hydration reactions take place. Moreover, during these reactions, the increase in the areas of contact between the particles leads to a reduction of porosity [23]. The optimal mixing time varied so that the fastest granulation (700 s) was obtained when carbon residue, cement, and metakaolin were mixed with KOH (CR3) whereas obtaining granules CR2 and CR4 with NaOH solvent took 300 sec longer. The longer granulation time led to larger granules. The amount of solvent was also tested, and it was found that the optimal solvent to carbon ratio was 1.2. Higher amounts of solvent resulted in deformation of the granule. For all the tested composite granules, the compressive strength increased with the time indicating that longer curing time promotes strength. However, the most stable and durable structure was obtained when acid washed carbon residue was mixed with CaO, metakaolin, and NaOH (CR2). The strength enhancement is probably due to the formation of calcium carbonate ($CaCO_3$), which forms via reactions 2 and 3 [43]:

$$CaO + H_2O \rightarrow Ca(OH)_2 \quad (2)$$

$$Ca(OH)_2 + CO_2 \rightarrow CaCO_3 + H_2O \quad (3)$$

However, metakaolin, is highly reactive [44] and can further react with $Ca(OH)_2$ (Eq. 2) forming, for example, calcium silicate hydrate gel and calcium aluminate silicate hydrate [45] resulting in increased strength. When NaOH is used, the mechanically strong product typically formed with metakaolin in general form is $2SiO_2 \cdot Al_2O_3 \cdot Na_2O \cdot 2H_2O$ [46]. XRD measurement was conducted to study possible hydration products. Results showed mostly similar structures for all the composite granular samples that can explain the different stabilities observed earlier (Table 2). However, as the samples were a mixture of four different components rather than

two, the expected changes were found in these complex phases when compared to others' research [45, 46]. Moreover, as the materials used were amorphous or semi-amorphous, it is known that the hydration products do not have very clear diffraction peaks but rather a "hump" that can be found between 20° and 30° 2θ [47-49]. In addition, the overlapping of peaks between hydrated and anhydrous compounds is likely. Fig. 1 shows as an example the X-ray diffractograms of CR, CR2, and CR3, where the "hump" can be seen between 20° and 30° 2θ.

The crystalline phases shown in this figure are identified as $Al_2(SO_4)(OH)_4 \cdot 3H_2O$ (JCPDS: 00-059-0397), SiO_2 (JCPDS: 01-070-2517), K_2SO_4 (JCPDS: 00-005-0613), $CaCO_3$ (JCPDS: 01-078-3262), $Ca_4Al_2(CO_3)(OH)_{12}(H_2O)_5$ (JCPDS: 04-011-4223), and Na_2CO_3 (JCPDS: 04-009-8633). For all of the samples, at least five reflections were detected. The first four crystalline phases mentioned were found from composite CR3, and the last two, as well as silicon oxide, were found from composite CR2. Only the $CaSO_4$ (JCPDS: 00-045-0157) crystalline phase was detected from CR. The observed difference between the crystalline signals of these two composite samples was expected as the binders used were different; that is, CR3 included cement, a mixture of Portland cement and blast furnace slag. As the results show, the composite materials were mostly carbonate-based hydration products, which together with the possible amorphous materials are expected to result in increasing strength in these samples, supporting the results from the mechanical strength test. For CR4, the results were similar those for CR2 and CR3 (data not shown).

3.2 Characterizations of the stable composite granules

3.2.1 Elemental analysis and morphology of the samples

The most stable materials were further characterized by elemental analyzer (C and O) and ICP-OES to evaluate their catalytic properties. Table S3 shows that agglomeration with binders introduced higher mineral content in all the composite granules (CR2 to CR4), such as oxygen (11–15%) and calcium (14–18%), with little Al (about 2%), Na (about 0–6%), K (about 1–9%), S (about 0–2%), and Si (about 3–4%). All the elemental contents within the composite granules were very similar, and the observed differences, such as in the amounts of sodium and potassium, between the samples were directly related to the different preparation methods used. Compared to the composite granules, CR contained the highest amount of carbon (75%) and the lowest heteroatom content: about 4% of oxygen, about 2% of sulfur and less than 1% altogether of Ca, Al, Na, K, Si, and Fe.

The FESEM images on the surface of CR and CR4 are presented in Fig. 2, and they were in good agreement with ICP-OES. The layered, quite homogenous structure of CR (Fig. 2 a) and the heterogeneous surface of the CR4 samples (Fig. 2 b) occupied with metal particles (< 1 μm) can be clearly seen.

3.2.2 Surface functional groups, basicity, and pH_{pzc}

One of the main aims of this work was to study the relationship between the surface group characteristics and their influences on oxidizing BPA in CWPO. Therefore, TPD, Boehm titration, pH, and pH_{pzc} were studied, and the results are presented in Table 4.

The granules had more basic than acidic characteristics as the carbon residue was mixed with basic salt (CaO) and amphoteric/semi-amphoteric substances (metakaolin and cement). Moreover, the XRD results indicated basic components, such as carbonates, on the surface of CR2 to CR4. The basicity of the materials was studied with TPD measurement under carbon dioxide gas in the temperature range of 50 °C to 950 °C (Fig. 3).

All composite granules exhibited very high CO_2 adsorption capacity (about 10–15 mmol/g), with a broad desorption band found between 600 °C and 700 °C that is related to CO_2 desorbed from strong basic sites [50, 51]. Compared to CR (desorption band maxima found around 800 °C), the composite granules exhibited more than 5 to 7 times higher uptake of CO_2. The basicity of the composite granules was depicted as arising mostly from the hydration products, described in section 3.1. Other oxygen-containing functionalities, such as chromene, pyrone, and quinones, have also been recognized to result in basicity of carbon materials [52-54]. However, the contribution of these functionalities is not yet fully understood [30, 33, 38, 53]. Based on these results, it was obvious that the composite granules had a basic surface, but CR also had some basic properties. The basicity of the samples decreased in the order CR2 > CR3 > CR4 > CR.

The variation in the number of acidic surface groups was determined with Boehm titrations that were found to support the interpretations arising from the TPD analysis (Table 4). Within the composite granules, the lowest number of acidic groups detected were found from CR2, which corresponds well with the highest amount of basicity detected by TPD. The results showed that the granulation treatment decreased the acidity as the composite granules had fewer acidic groups than CR. All the composite granules contained mainly lactonic groups, but for CR3, carboxylic groups were also detected. However, none of the composite granules contained phenolic groups. Compared to the composite granules, the surface of CR consisted similarly of lactonic groups, but carboxylic and phenolic groups were also detected. The difference in the acidic surface group content between the composite granules and CR was expected, as the composite granules contained basic/amphoteric binder agents and approximately 30% less carbon material than CR. However, Boehm titration has been shown to account only for 50% of the total oxygen content of carbon, and therefore, this method might result in misestimated values of the total surface chemical groups [38, 55]. The pH_{pzc} values were quite similar between the granules, and the values were higher than those detected from CR (Table 4). Similarly to pH_{pzc}, the pH values were observed to be higher in the composite granules than in CR, confirming the high basic nature of the materials. To summarize, the TPD, Boehm titration, pH, and pH_{pzc} results were in good agreement with the XRD results, confirming the higher basic characteristics of the composite granules compared to CR, which presumably could be beneficial for the CWPO reaction of BPA [12, 53].

3.2.3 Spectroscopic studies

DRIFT spectra were used to qualitatively identify the effects of the prepared granule treatment on the carbon surface structure. For this purpose, the spectrum of acid washed CR was used as a reference. The spectra were recorded between 4000 and 400 cm^{-1}. In all samples, broad peaks at around 3400–3500 cm^{-1} and 2300 cm^{-1} were detected which are typically assigned as stretching of the O-H bond of the surface hydroxyl groups and carbon dioxide, respectively (data not shown) [56]. As can be seen in Fig. 4, the highest intensity bands belong to the prepared composite granules, and the lowest intensity bands are in the CR, indicating that CR has fewer groups on the surface than composite granules CR2 to CR4. All the composite granules showed similar characteristics differing mainly only by the intensity level detected.

The composite granules retained some characteristic functional groups of the starting material; the peak around 1150 cm^{-1} was the strongest based on intensity. A broad band in granules at around 900–1150 cm^{-1}, with the maximum centered at 1000 cm^{-1}, and 1075–1250 cm^{-1} (maximum at 1150 cm^{-1}) in CR, has been assigned to C-O stretching in acids, alcohols, phenols, and esters, as well as C-O-C symmetric stretching in chromene, pyrones, and ether structures [57-60]. In addition, amorphous silica, which was detected with XRD in every composite granule (Fig. 1), having peaked typically around 1000–1100 cm^{-1} [56, 61], could be assigned within this 900–1150 cm^{-1} range. However, bands in this region are difficult to assign due to the overlapping of broad bands. The strong band at 1450 cm^{-1} observed in the spectrum of the composite granules can be assigned to the carbonates and O-H bending band. However, the XRD results showed that the granules were found to contain carbonate species (Fig. 1), no phenols were detected with Boehm titration (Table 4), and in the CR spectrum, no peak was observed in this region. Therefore, it was proposed that this peak corresponds to carbonates. In addition, these results confirmed the results of the elemental (Table S3) and EDS analysis that more oxygen-containing groups were introduced on the surface during the granulation process. Based on the intensity, at 1000 cm^{-1} the order of the highest peaks for the composite granules is CR2 > CR4 > CR3, whereas at 1450 cm^{-1} the order is CR4 > CR3 > CR2. The bands below 880 cm^{-1} are typical of deformation vibrations of C-H groups (out-of-plane) in benzene structures [56, 60].

XPS measurement was conducted to study the chemical structure of different samples in more detail. The following surface carbon species were considered: aromatics and aliphatics, single C-O/C-O-C bonds, double C=O/O-C=O bonds, and $\pi - \pi^*$ in aromatic ring or carbonate. Four oxygen groups, carbonyl or quinone oxygen (C=O), lactonic oxygen or anhydride oxygen (C-O-C), and carboxyl oxygen (COOH) and adsorbed water, were identified. Table 5 and Table 6 show the binding energies and atomic abundances obtained from the C1s and O1s fittings [46, 59, 62, 63].

The granulation treatment significantly altered the surface chemistry of composite granules when compared to the CR, but within the composite granules, the changes were not as drastic but at the same level. A similar trend was also observed earlier with DRIFTS (Fig. 3). The atomic composition data in Table 5 indicate that within the composite granules the C-O, C-O-C, and C=O/O-C=O content is lowest whereas there are more aromatics, aliphatics, and carbonates. C=O and O-C=O bonds can be presented as surface carbonyl, carboxylic groups, or pyrone structures [55]. Carboxyl groups were also found for CR and CR3 with Boehm titration (Table 4), whereas according to the DRIFTS results, no carbonyl or carboxyl acid was detected from any of the samples. This might be due to the different preparation methods as before the DRIFTS measurement, the powdered carbon must be diluted with KBr, which might have an effect on the detection limit. In addition, when complex samples are used, analysis with infrared becomes more difficult because each band may include contributions from different groups. In contrast, in the case of CR2 and CR4, no carboxyl acids were detected with Boehm titration (Table 4). This could be due to the narrower pore size (Table 2) detected from CR2 and CR4 that may hinder the titration of chemical groups detected elsewhere [64]. However, the changes between the samples observed in the O1s fitting (Table 6) showed that the relative amount of oxygen increased significantly in granules when compared to CR, that is, from 7.4% on CR to 40.3% on CR2, to 40.3% on CR3, and to 36.9% on CR4, a result supported very well by DRIFTS (Fig. 4; broad peaks around 900–1200 cm^{-1} and 1350–1550 cm^{-1}). These results are consistent with the elemental analysis (Table S3) results. Within the granules, CR2 and CR4 present similar surface characteristics (Table 5 and Table 6). Moreover,

the possibly identified lactonic groups from the O1s fitting support the information gained previously from Boehm titration (Table 4) where mainly these groups exist in all samples.

It was expected that during the curing and hardening of the composite granules, new bonds would form between the carbon material and the binders. Therefore, aluminum, silica, calcium, and potassium XPS 2p spectra and the sodium XPS 1s spectrum were measured from the composite samples. All the metals showed strong peaks in the XPS scan. The lowest atomic abundance found for all the materials was calcium (1.1–1.9%), and the highest amounts for sodium (10.4–10.7% for CR2 and CR4), silica (5.3–8.9%), and aluminum (2.7–6.0%) species. CR3 had the highest number of different metal oxygen species on its surface, whereas the content in the CR2 and CR4 samples were found to be lower and at a similar level, supporting again the previous results from elemental analysis and ICP-OES (Table S3). The binding energies may be associated with the following chemical species: 74.7–75.7 eV, Al_2O_3 and/or $Al(OH)_3$ [65, 66]; 102.8–103.6 eV, $Al_2Si_2O_5(OH)_4$ [67] and/or SiO_2 [68]; 347.5–348.3 eV, $CaCO_3$ [69]; 1073.3–1073.7 eV, Na_2O [70, 71]; and 293.8 eV, CH_3COOK [72]. However, the atomic abundances for these possible metal-oxygen complexes is low when compared to the amounts of carbon or oxygen detected. Therefore, catalytically active sites are not believed to be diminished due to these complexes. The alkaline reaction conditions have been shown to be beneficial in the CWPO reaction, and metal-oxygen complexes may create the basic environment needed for efficient decomposition of H_2O_2 [12]. Fig. 5 shows, as an example, the fittings of Al2p (BE 74.7 eV), Si2p (BE 102.8 eV), and Ca2p3 (BE 347.5 eV) and Ca2p1 spectra of sample CR3.

To conclude, the granulation produces strong changes in the surface chemistry of composite granules when compared to CR. The most significant changes introduced by the granulation treatment are the development of possible metal-oxygen and oxygen functionalities, such as calcium carbonates, aluminum oxides, and the chromene type of structures that supports the observed basicity of the carbon surface.

3.3 Catalytic wet peroxide oxidation studies

Principal aim was to prepare granular composite catalyst materials with sufficient mechanical strength. The more specific objective was to investigate the surface properties of the catalysts to understand the functionality of the surface and catalytic activity. Therefore, preliminary oxidation experiments were run, and the catalytic activity of the prepared materials was studied on BPA oxidation under CWPO experiments. Before the catalytic studies, the adsorption of BPA was checked (60 mg/L BPA was stirred with 1 g/L catalyst at 50 °C for 3 h) for all the materials. The conversion of BPA and TOC achieved with each sample upon CWPO after 3 h reaction time is given in Fig. 6.

Based on the adsorption results, the adsorption of the catalysts toward BPA decreased in the order CR > CR4 > CR3 > CR2, varying from 99% to 14%. All granular composite catalysts yielded significantly lower adsorption when compared to CR. The adsorption of BPA onto the materials is mainly related to the specific surface area of the samples (Table 2), as well as the pH of the reaction media. The high SSA, and porosity (especially macroporosity), was found to favor the removal of BPA by adsorption (CR and CR4). However, the pH of the reaction media is also known to affect the adsorption process [73]. At pH 6.2–5.4, the surface of CR is negatively charged ($pH > pH_{pzc}$, Table 4) resulting from the dissociation of the carboxylic, phenolic, and lactonic groups detected with Boehm titration, and should not favor adsorption of BPA as BPA is in molecule form below pH 8 [74]. Therefore, the adsorption of BPA onto

CR cannot be controlled only by the electrostatic interactions. The adsorption of phenolic compounds has been shown to be partly physical and partly chemical [75]. For example, hydrophobic $\pi - \pi$ interactions have been shown to increase BPA adsorption [74]. For the composite granules, the surface was found to be positively charged as the pH of the solution was lower than the zero point charge (Table 4), presumably resulting from the possible pyrone or chromene type of oxygen complexes on the surface (detected with XPS and DRIFTS; see section 3.2.3). Under these reaction conditions (pH > 8), BPA is in the deprotonated form (bisphenolate anion), thus favoring the electrostatic interaction [74]. However, relatively little adsorption was discovered. The lower adsorption can be partly explained by the lower SSA of the granules. In addition, the oxygen content on the surface of the composite granules was significantly higher compared to CR, which has been shown to decrease carbon hydrophobicity as the water molecules from the solution are bound to these surface oxygen species, thus reducing the accessibility of the BPA entry into the pores of carbon [75, 76].

All the composite catalysts showed similar BPA conversion (about 58–65%), but when adsorption was included, the best catalytic activity in terms of the BPA (about 50%) and TOC (about 48%) conversions was found when the CR2 catalyst was used. Based on the TPD results (Table 4), CR2 had the highest basicity observed compared to CR3 and CR4. Moreover, the CR2 catalyst had the lowest number of acidic surface oxygen groups (i.e., lactones) based on the Boehm titration results (Table 4) when compared to the other two catalysts. The basic surface characteristics in particular were observed to have a positive effect on the catalytic performances of the carbon materials in CWPO as basic sites act as active sites for faster catalytic decomposition of H_2O_2 during the CWPO process, whereas acidic sites inhibit the reaction [2, 12, 32, 77]. Moreover, other researchers [12] have shown that basic conditions are favored either in the reaction media or on the carbon surface. During the oxidation reaction, the pH of the reaction media for all the granules was at a similar level, varying between 9.7 and 10.7. The dissolved oxygen content was also investigated, and within the first hour of the reaction, the amount of dissolved oxygen dropped rapidly (about 10 mg O_2/L → 7.5 mg O_2/L), and then the level stabilized to 7.5–8.5 mg O_2/L, indicating that H_2O_2 was decomposed completely, and no excess oxygen was available. Therefore, as there were no statistically significant differences in the pH or dissolved oxygen levels between the granular composite catalysts, these results indicate that the possible higher amounts of basic functionalities, such as chromene and pyrone detected with DRIFTS and XPS (section 3.2.3), on the surface of CR2 led to more efficient BPA and TOC conversions.

CR4 catalyst was found to be as active a catalyst as CR2 with TOC conversion (48%). However, adsorption of BPA was found to be twice as high into CR4 (31%) than into CR2 (14%). The difference in adsorption capacity presumably originates from the higher SSA found on CR4. The lower TOC conversion (29%) observed for the CR3 catalyst might result from its slightly different porosity profile (Table 2) as wider pores have been shown to reduce the decomposition of H_2O_2 [12]. Moreover, CR3 had more acidic groups on its surface than the CR2 and CR4 catalysts (Table 4), which have been shown to hinder H_2O_2 decomposition by suppressing the dissociation of H_2O_2 [2, 12, 77].

For CR, the pH level during the reaction was different. The pH was more acidic compared to the basic conditions found with the granules; nevertheless, the pH level remained quite stable, varying between 6.2 and 5.4, whereas similarly to the granules, the dissolved oxygen level at first dropped from 9.9 mg O_2/L to 6.6 mg O_2/L after 1 h reaction time after which the level started to rise again ending up at 7 mg O_2/L. According to the TPD, XPS, and DRIFTS (Table 4 and section 3.2.3) results, CR had the lowest basicity detected. Therefore, as shown in Fig.

6, it can be concluded that the reaction was mainly governed by adsorption and not by oxidation.

According to the TOC measurements of the final samples, the formation of by-products during the oxidation reaction cannot be neglected, as the removal of organic compounds was not as high as the abatement of BPA during CWPO of BPA (Fig. 6). For example, CR2 catalyst, the BPA conversion was 65% and the TOC conversion was 48% while the theoretical TOC conversion should have been higher than 80%. One possible explanation for the low TOC conversion could be the batch-type reactor used in this study, which has been reported to result in a higher concentration of intermediate products [78].

3.3.1 Stability and leaching studies

The stability of CR2 after two consecutive CWPO experiments is summarized in Fig. 7. In the absence of H_2O_2, the BPA conversion was around 10% after 3 h, in contrast to the BPA and TOC conversions (first run) of around 47% and 50%, respectively. When CR2 was reused, its catalytic activity was found to be even higher than in the first run. The BPA and TOC conversions were approximately 10% higher than during the first run, indicating that no significant catalyst deactivation occurred. Moreover, the reaction occurred significantly faster during the second run. Presumably, the higher catalytic activity during the second run could partly have been due to the immobilized and concentrated BPA species filled inside the pores of the CR2, left from the first run, that were more efficiently oxidized than the BPA species from the more dilute solution. As the nonselective hydroxyl radical (·OH), formed via H_2O_2 decomposition, is close to the high concentration target organics near the carbon surface, it has been shown to favor high transformation efficiency and faster reaction kinetics than in Fenton oxidation in dilute aqueous systems [79]. Similar results have been presented elsewhere [5, 6]. The small dip in the TOC conversion on the second run observed between the measurement points of 120 and 180 min was related to the temporary reduction of the H_2O_2 concentration as the final dose of H_2O_2 was added at 120 min. However, as can be seen from Fig. 7, after the dip at 150 min, the TOC conversion level started to rise again, indicating there were enough reactive species left in the reaction.

The leaching of all the granules during the oxidation reactions was examined, and the possible leached metals (Ca and Al) were measured with ICP-OES. Calcium leached about 2 mg/L, but the aluminum concentration were found to be higher and to vary more, from 5 to 9 mg/L. From the point of view of catalytic activity, these metals are not active in CWPO, and therefore, the homogeneous catalysis can be neglected. The stability was also studied with the mass loss during the reaction, and the mass loss was found to be quite stable. However, approximately 30% of the catalyst weight was lost during the oxidation reaction.

To summarize catalytic studies, CR2, a granular composite catalyst prepared by combining acid washed carbon residue, metakaolin, and CaO with NaOH, was found to be the most catalytically active catalyst material in CWPO of BPA with the TOC and BPA conversions. The two other granular composite catalysts, CR3 and CR4, were prepared using acid washed carbon residue or carbon residue that was not acid washed, cement, metakaolin, and either KOH or NaOH, respectively. According to the TOC conversion, CR4 was nearly as active as CR2 whereas CR3 showed significantly lower catalytic activity. The difference between the catalytic activity of the granular composite catalysts was presumably mainly due to the different surface functionalities as the pH during the reaction was similar within the catalyst materials. In the case of CR, the oxidation reaction was found to be negligible, and the reaction

favored adsorption instead. From the point of view of the stability of the catalyst materials, it was found that the materials leached some metals, but also part of the material weight was lost due to the breakage of the granules.

4 Conclusion

Biomass-based carbon was granulated together with binder materials (metakaolin, cement, and CaO) at room temperature to produce porous and stable composite materials for catalytic water phase applications. The prepared composites were mechanically strong with porous structure. All the composites were found to be highly basic, containing only a few acidic functional groups detected with Boehm titration. The granulation process increased the oxygen species on the surface of the composite catalysts. All these findings were found to result positively toward CWPO. Preliminary results from the oxidation experiments indicated that the composite catalysts, even without impregnation of an active metal (e.g., Fe or Mn) on the catalyst surface, were active in the removal of BPA from aqueous solution, and approximately 25–50% abatement was achieved after the 3 h CWPO reaction. The most catalytically active composite catalyst, CR2, was prepared by combining acid washed carbon residue, metakaolin, and CaO with NaOH. This catalyst had the highest mechanical strength and basicity and the lowest concentration of acidic surface groups, carbonates, and metal-oxygen complexes. Characteristics were assumed to be the reason for the highest catalytic activity obtained with the CR2 material. To conclude, mechanically strong composite materials can be produced by combining biomass-based wood wastes with non-cementous materials, such as metakaolin. New granulated biomass-based carbon composite materials may be a promising technology for catalytic water treatment processes.

Acknowledgments

Financial support from Fortum foundation is gratefully acknowledged. The authors thank Mr. Jaakko Pulkkinen, Mr. Tuomo Vähätiitto, the staff at Trace Element Laboratory and at the Center of Microscopy and Nanotechnology, at the University of Oulu for their assistance with the elementary and XPS analysis, respectively. Lore Boets, Jere Taipalus and Eemeli Koskela are acknowledged.

References

[1] A. Bach, R. Semiat **The role of activated carbon as a catalyst in GAC/iron oxide/H2O2 oxidation process.** Desalination, 273 (2011), 57-63.

[2] F. Lücking, H. Köser, M. Jank, A. Ritter **Iron powder, graphite and activated carbon as catalysts for the oxidation of 4-chlorophenol with hydrogen peroxide in aqueous solution.** Water Res., 32 (1998), 2607-2614.

[3] A. Rey, M. Faraldos, J.A. Casas, J.A. Zazo, A. Bahamonde, J.J. Rodríguez **Catalytic wet peroxide oxidation of phenol over Fe/AC catalysts: Influence of iron precursor and activated carbon surface.** Appl. Catal. B-Environ., 86 (2009), 69-77.

[4] J.A. Zazo, J.A. Casas, A.F. Mohedano, J.J. Rodríguez **Catalytic wet peroxide oxidation of phenol with a Fe/active carbon catalyst.** Appl. Catal. B-Environ., 65 (2006), 261-268.

[5] J.R. Kim, S.G. Huling, E. Kan **Effects of temperature on adsorption and oxidative degradation of bisphenol A in an acid-treated iron-amended granular activated carbon.** Chem. Eng. J., 262 (2015), 1260-1267.

[6] E. Kan, S.G. Huling **Effects of Temperature and Acidic Pre-Treatment on Fenton-Driven Oxidation of MTBE-Spent Granular Activated Carbon.** Environ. Sci. Technol., 43 (2009), 1493-1499.

[7] Z. Liu, H. Meng, H. Zhang, J. Cao, K. Zhou, J. Lian **Highly efficient degradation of phenol wastewater by microwave induced H2O2-CuOx/GAC catalytic oxidation process.** Sep. Purif. Technol., 193 (2018), 49-57.

[8] I.F. Mena, E. Diaz, J.J. Rodriguez, A.F. Mohedano **CWPO of bisphenol A with iron catalysts supported on microporous carbons from grape seeds activation.** Chem. Eng. J., 318 (2017), 153-160.

[9] M. Al Bahri, L. Calvo, M.A. Gilarranz, J.J. Rodriguez, **Activated carbon from grape seeds upon chemical activation with phosphoric acid: Application to the adsorption of diuron from water.** Chem. Eng. J., 203 (2012), 348-356.

[10] R. Juhola, A. Heponiemi, S. Tuomikoski, T. Hu, T. Vielma, U. Lassi, **Preparation of Novel Fe Catalysts from Industrial By-Products: Catalytic Wet Peroxide Oxidation of Bisphenol A.** Top. Catal., 60 (2017), 1387-1400.

[11] T. Zhang, W.P. Walawender, L.T. Fan, M. Fan, D. Daugaard, R.C. Brown **Preparation of activated carbon from forest and agricultural residues through CO2 activation.** Chem. Eng. J., 105 (2004), 53-59.

[12] L.B. Khalil, B.S. Girgis, T.A.M. Tawfik **Decomposition of H2O2 on activated carbon obtained from olive stones.** J. Chem. Technol. Biotechnol., 76 (2001), 1132-1140.

[13] M.J.P. Brito, C.M. Veloso, R.C.F. Bonomo, R.C.I. Fontan, L.S. Santos, K.A. Monteiro, K. A. **Activated carbons preparation from yellow mombin fruit stones for lipase immobilization.** Fuel Process. Technol., 156 (2017), 421-428.

[14] The European parliament and the council of the European Union (2008). Directive 2008/98/ec.,2008. http://eur-lex.europa.eu/legalcontent/EN/TXT/?qid=1472559001854&uri=CELEX:32008L0098.

[15] E. Auer, A. Freund, J. Pietsch, T. Tacke **Carbons as supports for industrial precious metal catalysts.** Appl. Catal. A Gen., 173 (1998), 259-271.

[16] K.L. Kadam **Granulation Technology for Bioproducts.** Drying Technol., 11 (1993), 675.

[17] S.M. Iveson, J.D. Litster, K. Hapgood, B.J. Ennis **Nucleation, growth and breakage phenomena in agitated wet granulation processes: a review.** Powder Technol., 117 (2001), 3-39.

[18] C.A. Toles, W.E. Marshall, M.M. Johns **Granular activated carbons from nutshells for the uptake of metals and organic compounds.** Carbon, 35 (1997), 1407-1414.

[19] W.C. Purnomo, D. Castello, L. Fiori **Granular Activated Carbon from Grape Seeds Hydrothermal Char.** Appl. Sci., 8 (2018), 331

[20] B. Pendyal, M.M. Johns, W.E. Marshall, M. Ahmedna, R.M. Rao **Removal of sugar colorants by granular activated carbons made from binders and agricultural by-products.** Bioresource Technol., 69 (1999), 45-51.

[21] B. Pendyal, M.M. Johns, W.E. Marshall, M. Ahmedna, R.M. Rao **The effect of binders and agricultural by-products on physical and chemical properties of granular activated carbons.** Bioresource Technol., 68 (1999), 247-254.

[22] M. Ahmedna, W.E. Marshall, R.M. Rao **Production of granular activated carbons from select agricultural by-products and evaluation of their physical, chemical and adsorption properties.** Bioresource Technol., 71 (2000), 113-123.

[23] E.M. Holt **The properties and forming of catalysts and absorbents by granulation.** Powder Technol., 140 (2004), 194-202.

[24] V.H. Dodson **Pozzolans and the Pozzolanic Reaction.** In: Concrete Admixtures, Springer, Boston MA, (1990), 159-201.

[25] P. Sazama, O. Bortnovsky, J. Dědeček, Z. Tvarůžková, Z. Sobalík, **Geopolymer based catalysts—New group of catalytic materials.** Catal. Today, 164 (2011), 92-99.

[26] H. Cheng, K. Lin, R. Cui, C. Hwang, T. Cheng, Y. Chang **Effect of solid-to-liquid ratios on the properties of waste catalyst–metakaolin based geopolymers.** Constr. Build. Mater., 88 (2015), 74-83.

[27] Q. Tang, Y. Ge, K. Wang, Y. He, X. Cui **Preparation and characterization of porous metakaolin-based inorganic polymer spheres as an adsorbent.** Mater. Des., 88 (2015), 1244-1249.

[28] J. Davidovits **Geopolymers - Inorganic polymeric new materials.** J. Therm. Anal., 37 (1991), 1633-1656.

[29] F. Rodríguez-Reinoso **The role of carbon materials in heterogeneous catalysis.** Carbon, 36 (1998), 159-175.

[30] J.L. Figueiredo, M.F.R. Pereira **The role of surface chemistry in catalysis with carbons.** Catal. Today, 150 (2010), 2-7.

[31] R.W. Coughlin **Carbon as adsorbent and catalyst.** Ind. Eng. Chem. Prod. RD., 8 (1969), 12-23.

[32] V.P. Santos, M.F.R. Pereira, P.C.C. Faria, J.J.M. Órfão **Decolourisation of dye solutions by oxidation with H2O2 in the presence of modified activated carbons.** J. Hazard. Mater., 162 (2009), 736-742.

[33] H. Hattori **Heterogeneous Basic Catalysis.** Chem. Rev., 95 (1995), 537-558.

[34] M.S. Kim, Y. Jun, C. Lee, J.E. Oh **Use of CaO as an activator for producing a price-competitive non-cement structural binder using ground granulated blast furnace slag.** Cement Concrete Res., 54 (2013), 208-214.

[35] T. Luukkonen, H. Runtti, M. Niskanen, E. Tolonen, M. Sarkkinen, K. Kemppainen, J. Rämö, U. Lassi **Simultaneous removal of Ni(II), As(III), and Sb(III) from spiked mine effluent with metakaolin and blast-furnace-slag geopolymers.** J. Environ. Manage., 166 (2016), 579-588.

[36] S. Brunauer, P.H. Emmett, E. Teller **Adsorption of Gases in Multimolecular Layers.** J. Am. Chem. Soc., 60 (1938), 309-319.

[37] N.A. Seaton, J.P.R.B. Walton, N. Quirke **A new analysis method for the determination of the pore size distribution of porous carbons from nitrogen adsorption measurements.** Carbon, 27 (1989), 853-861.

[38] H.P. Boehm **Surface oxides on carbon and their analysis: a critical assessment.** Carbon, 40 (2002), 145-149.

[39] M.V. Lopez-Ramon, F. Stoeckli, C. Moreno-Castilla, F. Carrasco-Marin **On the characterization of acidic and basic surface sites on carbons by various techniques.** Carbon, 37 (1999), 1215-1221.

[40] K. Somna, C. Jaturapitakkul, P. Kajitvichyanukul, P. Chindaprasirt **NaOH-activated ground fly ash geopolymer cured at ambient temperature.** Fuel, 90 (2011), 2118-2124.

[41] F.A. Memon, F. Nuruddin, S. Khan, N. Shafiq, T. Ayub **Effect of Sodium Hydroxide Concentration on Fresh Properties and Compressive Strength of Self-Compacting Geopolymer Concrete.**, JESTEC, 8 (2013), 44-56.

[42] J. Davidovits **Properties of geopolymer cements.** Proceedings First International Conference on Alkaline Cements and Concretes 1 (1994), 131-149.

[43] J. Pesonen, V. Kuokkanen, T. Kuokkanen, M. Illikainen **Co-granulation of bio-ash with sewage sludge and lime for fertilizer use.** J. Environ. Chem. Eng., 4 (2016), 4817-4821.

[44] C. Poon, L. Lam, S.C. Kou, Y. Wong, R. Wong **Rate of pozzolanic reaction of metakaolin in high-performance cement pastes.** Cement Concrete Res., 31 (2001), 1301-1306.

[45] A. Gameiro, S.A. Santos, R. Veiga, A. Velosa **Hydration products of lime–metakaolin pastes at ambient temperature with ageing.** Thermochim. Acta, 535 (2012), 36-41.

[46] C. Li, H. Sun, A. Li **A review: The comparison between alkali-activated slag (Si+Ca) and metakaolin (Si+Al) cements.** Cement Concrete Res., 40 (2010), 1341-1349.

[47] R.P. Williams, A. van Riessen **Determination of the reactive component of fly ashes for geopolymer production using XRF and XRD.** Fuel, 89 (2010), 3683-3692.

[48] J.G.S. van Jaarsveld, J.S.J. van Deventer **Effect of the Alkali Metal Activator on the Properties of Fly Ash-Based Geopolymers.** Ind. Eng. Chem. Res., 38 (1999), 3932-3941.

[49] M. Criado, A. Fernández-Jiménez, A.G. de la Torre, M.A.G. Aranda, A. Palomo **An XRD study of the effect of the SiO2/Na2O ratio on the alkali activation of fly ash.** Cement Concrete Res., 37 (2007), 671-679.

[50] X. Song, K. Li, C. Wang, X. Sun, P. Ning, L. Tang **Regeneration performance and mechanism of modified walnut shell biochar catalyst for low temperature catalytic hydrolysis of organic sulfur.** Chem. Eng. J., 330 (2017), 727-735.

[51] G. Busca **Bases and Basic Materials in Chemical and Environmental Processes. Liquid versus Solid Basicity.** Chem. Rev., 110 (2010), 2217-2249.

[52] H.P. Boehm, M. Voll **Basische Oberflächenoxide auf Kohlenstoff—I. Adsorption von säuren.** Carbon, 8 (1970), 227-240.

[53] R.S. Ribeiro, A.M.T. Silva, J.L. Figueiredo, J.L. Faria, H.T. Gomes **Catalytic wet peroxide oxidation: a route towards the application of hybrid magnetic carbon nanocomposites for the degradation of organic pollutants. A review.** Appl. Catal. B-Environ., 187 (2016), 428-460.

[54] A. Contescu, C. Contescu, K. Putyera, J.A. Schwarz **Surface acidity of carbons characterized by their continuous pK distribution and Boehm titration.** Carbon, 35 (1997), 83-94.

[55] C.H. Tessmer, R.D. Vidic, L.J. Uranowski **Impact of Oxygen-Containing Surface Functional Groups on Activated Carbon Adsorption of Phenols.** Environ. Sci. Technol., 31 (1997), 1872-1878.

[56] F.I. Williams DH **Spectroscopic methods in organic chemistry**, 5th edn. McGraw-Hill publishing, Berkshire, **(**1995), 41-45.

[57] J.L. Figueiredo, M.F.R. Pereira, M.M.A. Freitas, J.J.M. Órfão **Modification of the surface chemistry of activated carbons.** Carbon, 37 (1999), 1379-1389.

[58] A. Barroso-Bogeat, M. Alexandre-Franco, C. Fernández-González, V. Gómez-Serrano **Activated carbon surface chemistry: Changes upon impregnation with Al(III), Fe(III) and Zn(II)-metal oxide catalyst precursors from NO3− aqueous solutions.** Arab. J. Chem. (2016) https://doi.org/10.1016/j.arabjc.2016.02.018.

[59] C. Moreno-Castilla, M.V. López-Ramón, F. Carrasco-Marín. **Changes in surface chemistry of activated carbons by wet oxidation.** Carbon, 38 (2000), 1995-2001.

[60] A. Reffas, V. Bernardet, B. David, L. Reinert, M.B. Lehocine, M. Dubois, N. Batisse, L. Duclaux **Carbons prepared from coffee grounds by H3PO4 activation: Characterization and adsorption of methylene blue and Nylosan Red N-2RBL.** J. Hazard. Mater., 175 (2010), 779-788.

[61] A. Hajimohammadi, J.S.J. van Deventer **Solid Reactant-Based Geopolymers from Rice Hull Ash and Sodium Aluminate.** Waste Biomass Valori., 8 (2017), 2131-2140.

[62] L. Prati, D. Bergna, A. Villa, P. Spontoni, C.L. Bianchi, T. Hu, H. Romar, U. Lassi **Carbons from second generation biomass as sustainable supports for catalytic systems.** Catal. Today, 301 (2018), 239-243.

[63] M. Walczyk, A. Świątkowski, M. Pakuła, S. Biniak **Electrochemical studies of the interaction between a modified activated carbon surface and heavy metal ions.** J Appl. Electrochem., 35 (2005), 123-130.

[64] M. Domingo-García, F.J. López Garzón, M.J. Pérez-Mendoza **On the Characterization of Chemical Surface Groups of Carbon Materials.** J. Colloid Interf. Sci., 248 (2002), 116-122.

[65] J.T. Kloprogge, L.V. Duong, B.J. Wood, R.L. Frost **XPS study of the major minerals in bauxite: Gibbsite, bayerite and (pseudo-)boehmite.** J. Colloid Interf. Sci., 296 (2006), 572-576.

[66] J. Zähr, S. Oswald, M. Türpe, H.J. Ullrich, U. Füssel **Characterisation of oxide and hydroxide layers on technical aluminum materials using XPS.** Vacuum, 86 (2012), 1216-1219.

[67] H. He, T.L. Barr, J. Klinowski **ESCA Studies of Framework Silicates with the Sodalite Structure. 2. Ultramarine.** J. Phys. Chem., 98 (1994), 8124-8127.

[68] B. Herreros, T.L. Barr, P.J. Barrie, J. Klinowski **Spectroscopic Studies of 5-Coordinate Silicon Compounds.** J. Phys. Chem., 98 (1994), 4570-4574.

[69] J.F. Moulder, W.F. Stickle, P.E. Sobol, K.D. Bomben **Handbook of X-ray photoelectron spectroscopy,** 2nd edn. Perkin-Elmer Corporation, Minnesota, **(**1992), 67-69.

[70] A. Barrie, F.J. Street **An Auger and X-ray photoelectron spectroscopic study of sodium metal and sodium oxide.** J. Electron Spectrosc., 7 (1975), 1-31.

[71] A.P. Savintsev, Y.O. Gavasheli, Z. K.H. Kalazhokov, K.H. Kalazhokov **X-ray photoelectron spectroscopy studies of the sodium chloride surface after laser exposure.** J. Phys. Conf. Ser., 774 (2016), 012118.

[72] R. Jerome, P. Teyssie, J.J. Pireaux, J.J. Verbist **Surface analysis of polymers end-capped with metal carboxylates using x-ray photoelectron spectroscopy.** Appl. Surf. Sci., 27 (1986), 93-105.

[73] L.R. Radovic, C. Mureno-Castilla, J. Rivera-Utrilla **Carbon materials as adsorbents in aqueous solutions.** Chem. Phys. Carbon, 29 (2001), 227-405.

[74] I. Bautista-Toledo, M.A. Ferro-García, J. Rivera-Utrilla, C. Moreno-Castilla, F.J.V. Fernández **Bisphenol A removal from water by activated carbon. Effects of carbon characteristics and solution chemistry.** Environ. Sci. Technol., 39 (2005), 6246-6250.

[75] C. Moreno-Castilla **Adsorption of organic molecules from aqueous solutions on carbon materials.** Carbon, 42 (2004), 83-94.

[76] R.W. Coughlin, F.S. Ezra **Role of surface acidity in the adsorption of organic pollutants on the surface of carbon.** Environ. Sci. Technol., 2, (1968), 291-297.

[77] L.C.A. Oliveira, C.N. Silva, M.I. Yoshida, R.M. Lago **The effect of H2 treatment on the activity of activated carbon for the oxidation of organic contaminants in water and the H2O2 decomposition.** Carbon, 42 (2004), 2279-2284.

[78] G. Centi, S. Perathoner, T. Torre, M.G. Verduna **Catalytic wet oxidation with H2O2 of carboxylic acids on homogeneous and heterogeneous Fenton-type catalysts.** Catal. Today, 55 (2000), 61-69.

[79] S.G. Huling, P.K. Jones, W.P. Ela, R.G. Arnold **Fenton-driven chemical regeneration of MTBE-spent GAC.** Water Res., 39 (2005), 2145-2153.

Figure captions

Fig. 1. Comparing X-ray diffractograms of CR, CR2 and CR3. Symbols are related to following compounds: x $CaSO_4$; = $Al_2(SO_4)(OH)_4 \cdot 3H_2O$; * SiO_2; ¤ K_2SO_4; + $CaCO_3$; # $Ca_4Al_2(CO_3)(OH)_{12}(H_2O)_5$; ! Na_2CO_3.

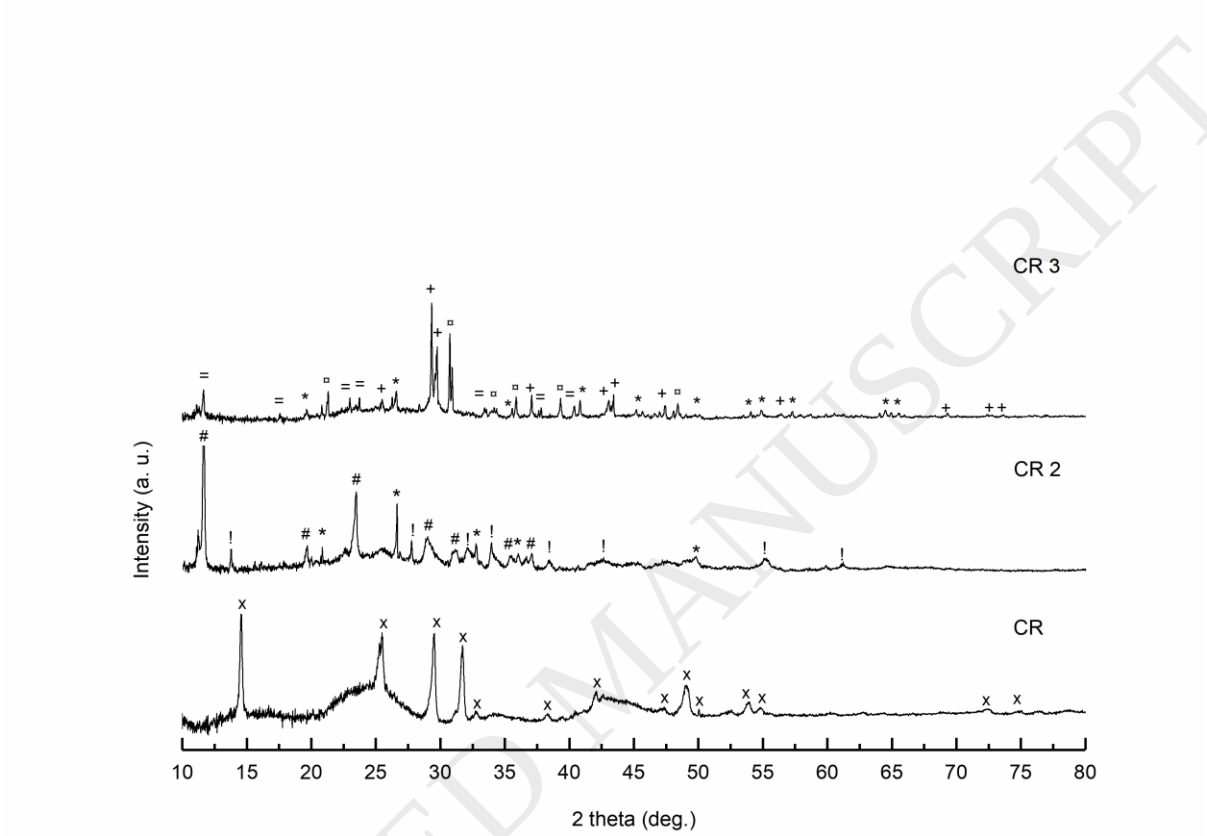

Fig. 2. FESEM images of CR (a) and CR4 (b) (magnification x 3000).

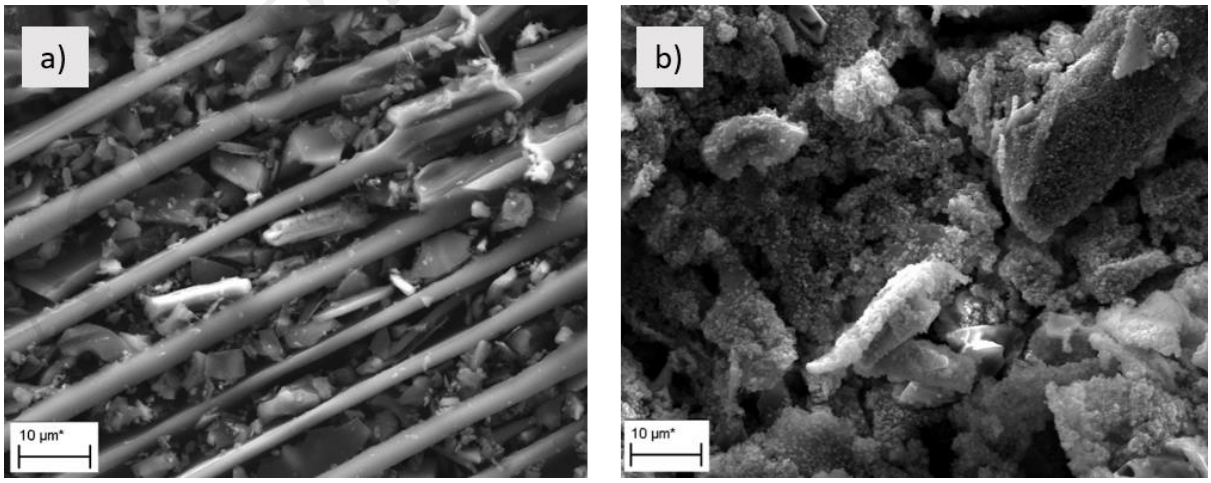

Fig. 3. Temperature programmed desorption of CO_2 patterns of CR and CR2-CR4 samples.

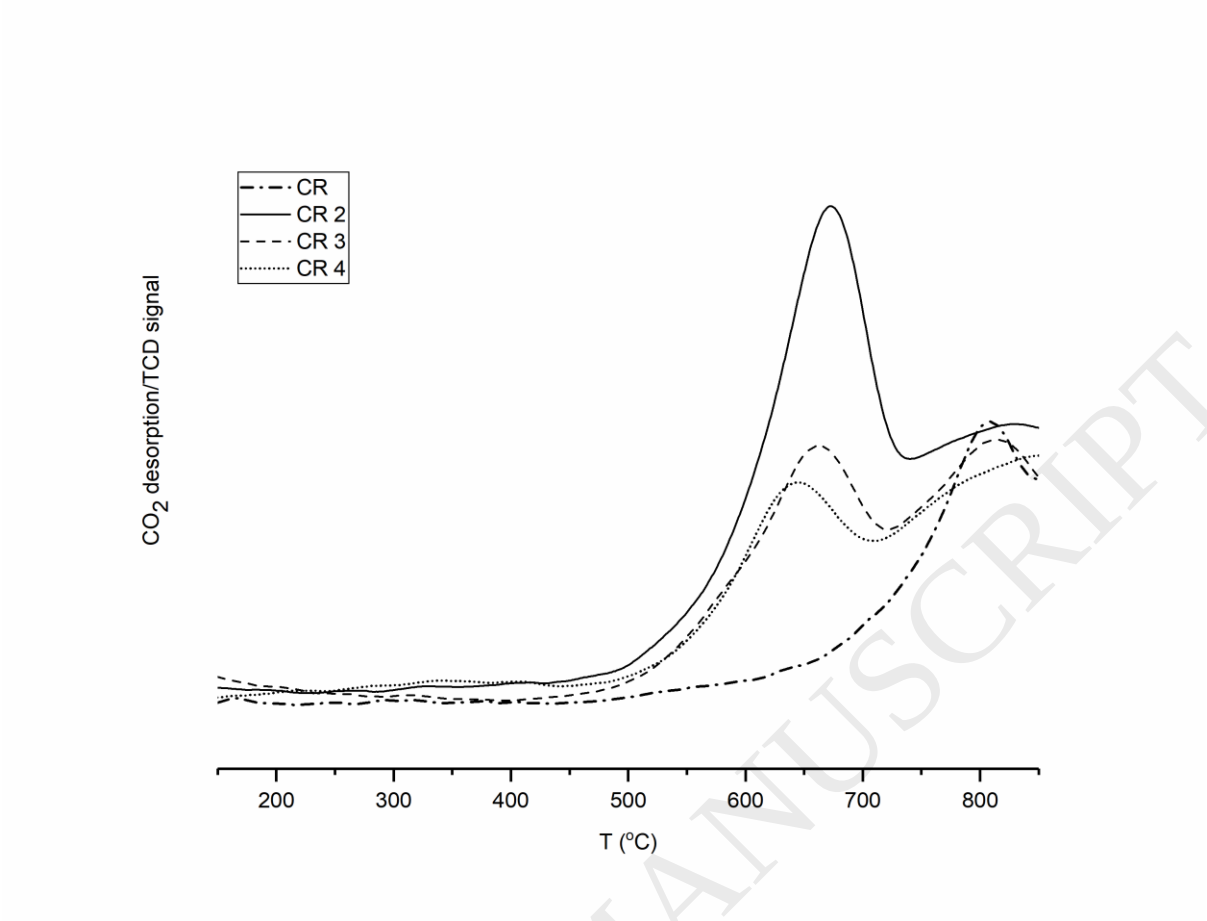

Fig. 4. DRIFTS spectra for acid washed carbon residue (CR) and granular composite catalysts (CR2- CR4) at 550-1700 cm^{-1}.

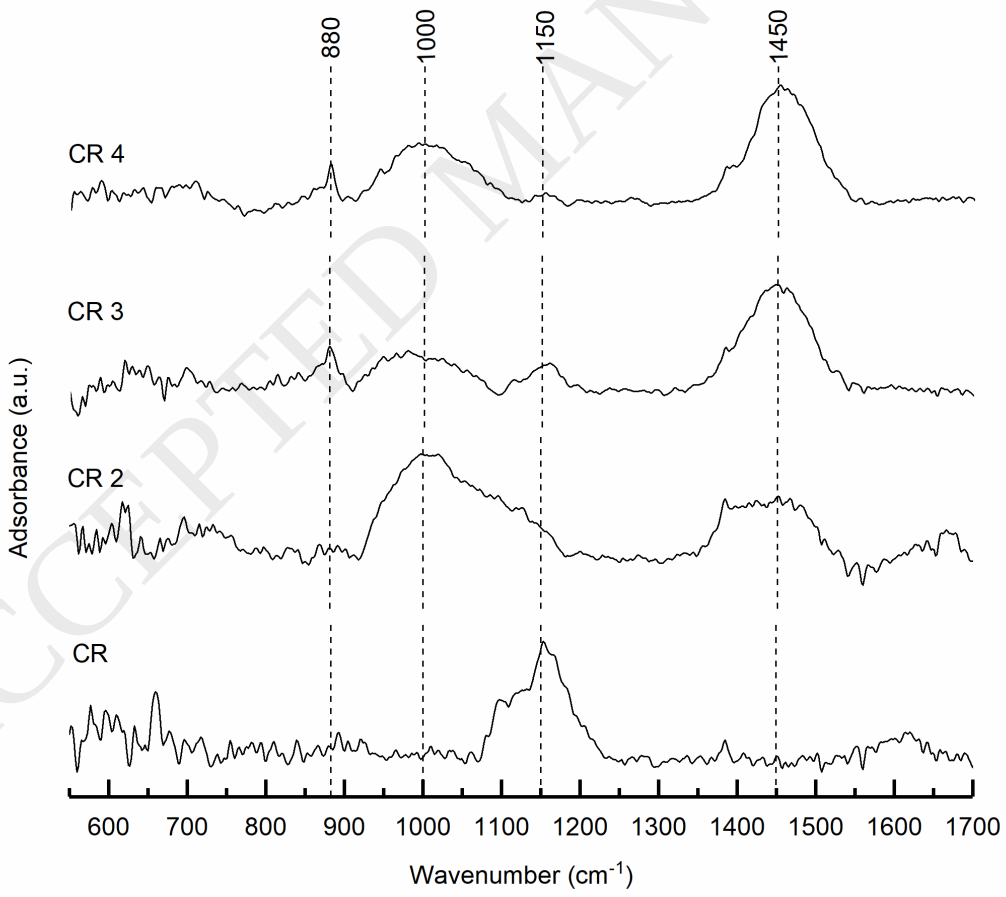

Fig. 5. XPS patterns of Al2p, Si2p and Ca2p of sample CR3.

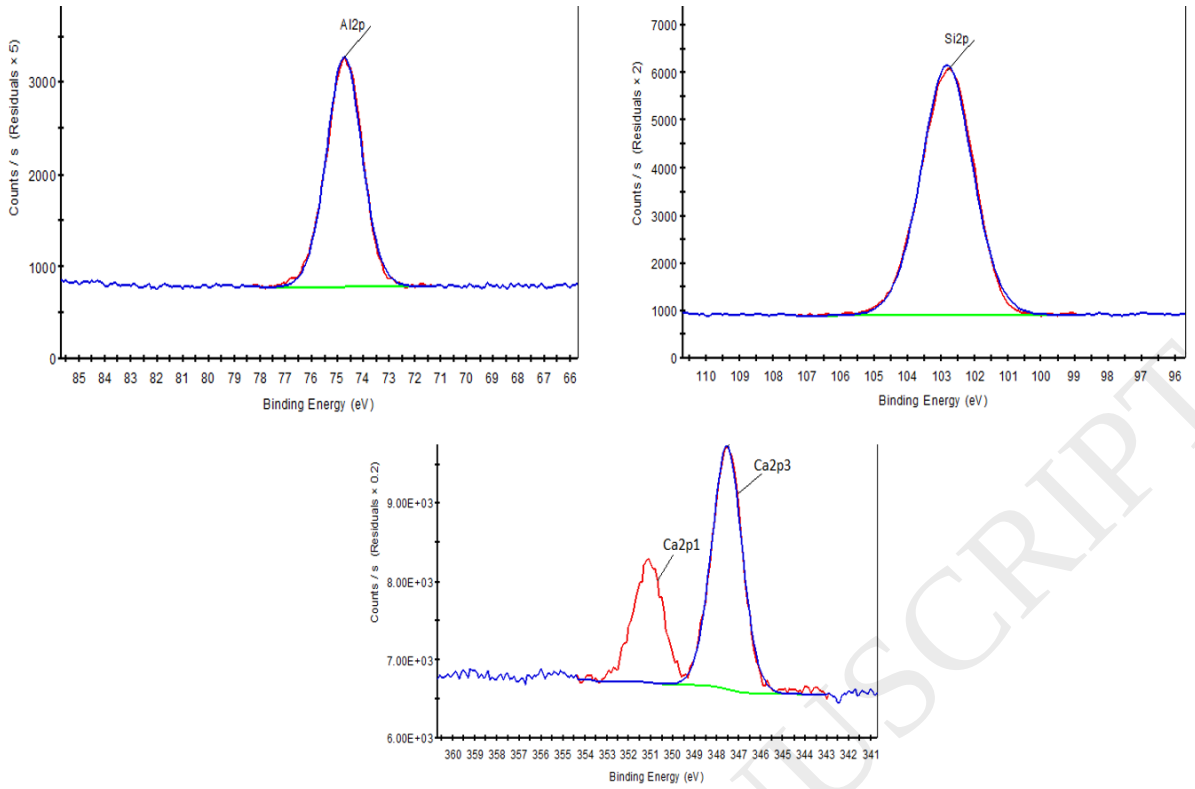

Fig. 6. Bisphenol A removal and TOC conversion after 3 h reaction (Reaction conditions: c(BPA)=60 mg/L, c(H2O2) = 1.5 g/L, c(catalyst) = 1 g/L, T = 50 ℃, initial pH for CR 5- 6.5, for CR2- CR4 pH 9-11).

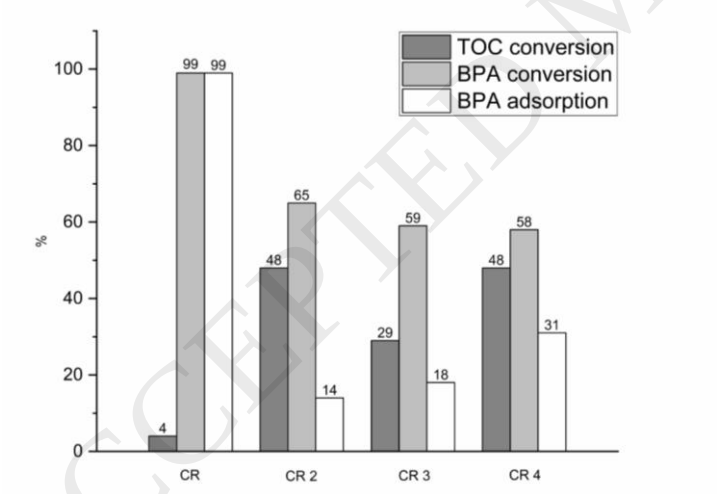

Fig. 7. BPA and TOC conversion of bisphenol A as a function of time of reaction (Reaction conditions: c(BPA)=60 mg/L, c(H_2O_2) = 1.5 g/L, c(catalyst) = 1 g/L, T = 50 ℃, initial pH 9-11) of granular composite catalyst CR2. The reused CR2 was filtered after first CWPO reaction, and prior to the second run, washed with deionized water and dried at 105 ℃ overnight.

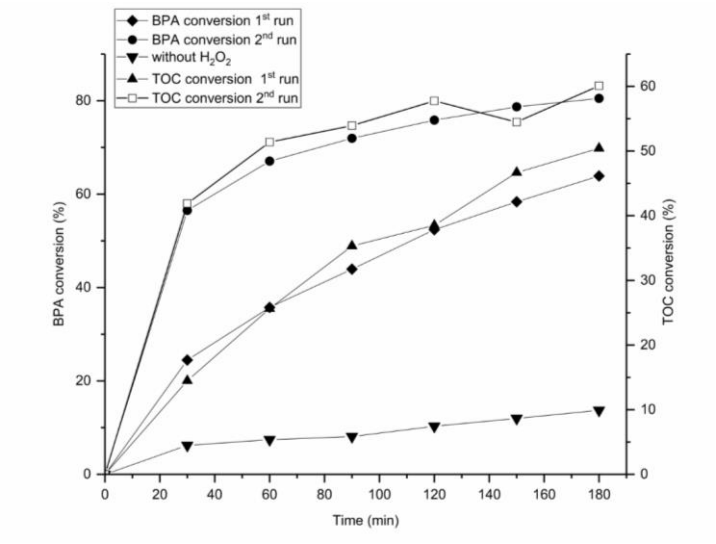

Table

Table 1. Combinations used in granulating experiments of willow carbon (CW) and carbon residue (CR).

Sample	Binding agents (1:1)*	Solvent (5 M)*	Mixing time (s)
CW 1	CaO + Metakaolin	KOH	700
CW 2	CaO + Metakaolin	NaOH	600
CW 3	Cement + Metakaolin	KOH	500
CW 4	Cement + Metakaolin	NaOH	500
CR1	CaO + Metakaolin	KOH	700
CR2	CaO + Metakaolin	NaOH	1000
CR3	Cement + Metakaolin	KOH	700
CR4	Cement + Metakaolin	NaOH	1000

*For all the granulations, the optimum binding agent to carbon ratio was 0.3 and the solvent to carbon ratio 1.2.

Table 2. Characteristics for the stable composite granules.

Sample	SSA	Pore size	Total pore volume	Micro	Meso	Macro	Mechanical Strength (N)			Solvent	Mixing time
	(m^2/g)	(nm)	(cm^3/g)	Porosity (%)			1	7	28(d)	(5 M)	(s)
CR	537	3.71	0.262	56	44	1	-	-	-	-	-
CR2	166	4.02	0.098	44	55	1	13	17	28	NaOH	1000
CR3	152	5.51	0.089	43	42	15	9	15	20	KOH	700
CR4	205	4.02	0.105	52	46	2	13	14	22	NaOH	1000

Table 4. Basicity and the surface chemical characteristics of CR and CR2-CR4 samples.

Sample	Basicity	The surface oxygen groups by Boehm's titration			pH_{pzc}	pH
	CO_2 uptake	Carboxylic groups	Lactonic groups	Phenolic groups		
	mmol/g	mmol/g	mmol/g	mmol/g		
CR	2.140	1.860	2.950	0.142	4.51	8.17
CR2	14.90	0.000	0.140	0.000	12.1	10.7
CR3	12.70	0.810	0.152	0.000	11.8	9.77
CR4	10.90	0.000	0.318	0.000	12.3	10.3

Table 5. XPS C1s spectra of CR and CR2- CR4. Binding energies and relative atomic contents.

Sample	Binding energy (eV) and the atomic abundance (%)			
	284.7-284.8	285.6-286.7	287.3-288.6	290-291.3
	Aromatics and aliphatics	C-O, C-O-C	C=O, O-C=O	$\pi - \pi^*$ in aromatic ring/carbonate, CO_2
CR	51.7	25.9	7.10	6.40
CR2	26.2	2.66	2.57	5.93

CR3	30.3	1.34	0.72	1.97
CR4	32.4	2.11	2.27	4.88

Table 6. O1s XPS O1s spectra of CR and CR2- CR4. Binding energies and relative atomic contents.

Sample	**Binding energy (eV) and the atomic abundance (%)**			
	531.4-531.8	**532.3-533**	**533.5-535.5**	**536.3-537.5**
	C=O, O-C=O	**C-O, C-O-C**	**COOH**	**H_2O**
CR	1.63	4.27	1.11	0.34
CR2	9.27	22.5	6.95	1.56
CR3	27.9	10.1	4.7	-
CR4	8.67	21.9	5.67	1.63